

The biennial life strategy in a random environment

J. B. T. M. Roerdink

Department of Applied Mathematics, Centre for Mathematics and Computer Science,
Kruislaan 413, 1098 SJ Amsterdam, The Netherlands

Abstract. A discrete-time population model with two age classes is studied which describes the growth of biennial plants in a randomly varying environment. A fraction of the oldest age class delays its flowering each year. The solution of the model involves products of random matrices. We calculate the exact mean and variance of the long-run geometric growth rate assuming a gamma distribution for the random number of offspring per flowering plant after one year. It is shown, both by analytical calculation and numerical examples, that it is profitable for the population to delay its flowering, in the sense that the average growth rate increases and the extinction probability decreases. The optimal values of the flowering fraction depend upon the environmental and model parameters.

Key words: Population biology — Random matrix products

1. Introduction

Strictly biennial plants are characterized by the fact that they flower only in the second year of their existence after which they die. Many biennial species, however, show the phenomenon of *delayed flowering*, meaning that they flower only in the third year or even later [8].

The biennial life strategy in a deterministic environment was discussed by Hart [6] and Van der Meijden and Van der Waals-Kooi [15]. Due to the fact that biennial plants reproduce only once every two years, a biennial has to produce four times as many seeds as a perennial and twice as many seeds as an annual plant to attain the same rate of increase, even in the most favourable situation. Thus it would seem that a biennial with an extended life span due to delayed flowering will be even worse off (unless the population was already in a state of decline before the delay).

The situation changes when the population grows in a randomly varying environment, especially when the average rate of increase of the population is low and the environmental fluctuations are large. This was shown by simulation studies of Klinkhamer and de Jong [8], who considered a model of a biennial species growing in a single, isolated habitat patch, without dispersal and without a seed bank, with all individuals dying after flowering. Their model, which applies

to the case of *density-independent* population growth, consists of the following pair of difference equations, where t is a time just before flowering:

$$N_{1,t+1} = f\phi_t N_{2,t} \quad (1.1a)$$

$$N_{2,t+1} = sN_{1,t} + (1-f)sN_{2,t} \quad (1.1b)$$

for $t = 0, 1, 2, \dots$, with:

- $N_{1,t}$ the number of individuals which are one year old at time t ;
- $N_{2,t}$ the number of individuals older than one year at time t ;
- s survival rate per year of individuals older than one year, $0 < s < 1$;
- f fraction of individuals older than one year that flowers in a given year, $0 \leq f \leq 1$;
- ϕ_t the number of offspring per flowering plant after one year, $\phi_t \geq 0$.

In the simulations all parameters were constants except $\{\phi_t\}$ which was assumed to be an independent identically distributed (i.i.d.) sequence of random variables, with $\phi_t = a \exp b\gamma_t$, a and b positive and γ_t uniformly distributed on $[0, 1]$. It was found that in a wide parameter range delayed flowering is profitable in two ways,

- (i) by increasing the long-run geometric growth rate;
- (ii) by reducing the extinction rate.

It is the purpose of the present paper to support these simulation results by presenting a number of exact analytical calculations pertaining to the model (1.1), based on the theory of random products of nonnegative matrices, see e.g. Cohen [3, 4], Heyde and Cohen [7] and Tuljapurkar [10-14]; for more general matrices see [2, 9]. In particular we study how the distribution of age-structure (or the ratio $N_{1,t}/N_{2,t}$), the mean and variance of the geometric growth rate and the probability of reaching an arbitrarily imposed extinction boundary depend upon the flowering fraction f . The exact results are used as a test of a number of commonly used approximations as discussed in [11].

The organization of the paper is as follows. In Sect. 2 we treat the growth of the average population. Section 3 summarizes the required results from the theory of random matrix products and contains the solution for the stationary age-structure distribution, assuming a two-parameter gamma distribution for ϕ_t . The mean growth rate is studied in Sect. 4. Also the behaviour of the variance of the growth rate is discussed. In Sect. 5 we give an asymptotic analysis of the mean growth rate, expressing the latter in terms of Kummer functions, for values of the flowering fraction near unity. The analytical approximations mentioned above are considered in Sect. 6. Section 7 contains a brief discussion of extinction probabilities and we summarize our results in Sect. 8.

2. Growth of the average population

By introducing the population vector $n_t = (N_{1,t}, N_{2,t})'$, where the prime denotes transposition, Eq. (1.1) assumes the form

$$n_{t+1} = X_t n_t \quad (2.1)$$

where X_t is the nonnegative matrix

$$X_t = \begin{pmatrix} 0 & f\phi_t \\ s & (1-f)s \end{pmatrix}. \quad (2.2)$$

Hence, denoting the initial population vector by n_0 ,

$$n_t = X_t X_{t-1} \dots X_1 n_0 \tag{2.3}$$

so that the long-term properties of n_t depend on the behaviour of the random matrix products $X_t X_{t-1} \dots X_1$, $t = 1, 2, \dots$. We assume $\{\phi_i\}$ to be an i.i.d. sequence with a common distribution to be specified below (Sect. 3).

Growth of the *average* population is easily studied, since

$$\mathbb{E}(n_t) = \{\mathbb{E}(X)\}^t n_0 \tag{2.4}$$

because of the i.i.d.-property of the matrices $\{X_i\}$. Here \mathbb{E} denotes the mathematical expectation with respect to the probability distribution of the random variable ϕ_i . The matrix

$$\mathbb{E}(X) = \begin{pmatrix} 0 & f\bar{\phi} \\ s & (1-f)s \end{pmatrix}, \quad \bar{\phi} = \mathbb{E}(\phi_i) < \infty \tag{2.5}$$

is primitive for $0 < f < 1$, assuming $\bar{\phi}$ to be positive. Hence each of the components of the average population vector grows geometrically for large t ,

$$\mathbb{E}(N_{i,t}) \sim C_i \lambda_0^t \quad (t \rightarrow \infty) i = 1, 2 \tag{2.6}$$

where the constants $\{C_i\}$ depend upon the initial conditions and

$$\lambda_0(f) = \frac{1}{2}[s(1-f) + \{s^2(1-f)^2 + 4f\bar{\phi}s\}^{1/2}] \tag{2.7}$$

is the largest eigenvalue of $\mathbb{E}(X)$. For $f = 0$ or $f = 1$ the matrix (2.5) is no longer primitive, but one easily verifies that (2.7) still describes the growth of the *total* population in those cases.

If $\bar{\phi}$ is identified with the number of offspring per plant in a *deterministic* environment it follows that the randomness of ϕ_i does not affect the growth of the average population. Furthermore it can be readily shown that

$$\frac{\partial \lambda_0}{\partial f} > 0 \quad \text{if } \bar{\phi} > s \tag{2.8a}$$

$$\frac{\partial \lambda_0}{\partial f} < 0 \quad \text{if } \bar{\phi} < s. \tag{2.8b}$$

Hence in the first case the average population grows at its largest rate when $f = 1$. Thus in a deterministic environment it is not profitable for a growing population, i.e. a population with $\lambda_0(1) = \sqrt{\bar{\phi}s} > 1$ (hence $\bar{\phi} > s$), to delay its flowering. This confirms the conclusions of [6, 15].

To summarize, we have seen that in a random environment the average population grows fastest when $f = 1$, as long as $\bar{\phi} > s$. However, it is characteristic of multiplicative systems of the type (2.1) that almost all solutions have a growth rate which in general is *strictly smaller* than the growth rate of the average population [10]. The study of this so-called *geometric* growth rate is the subject of the next sections.

3. The stationary age-structure distribution

First, we introduce some notation. For any vector $x \in \mathbb{R}_+^2 = \{(x_1, x_2) \in \mathbb{R}^2: x_1 \geq 0, x_2 \geq 0\}$ we define the *norm*

$$|x| = \sum_{i=1}^2 |x_i| \quad (3.1)$$

and a corresponding *unit vector* in the direction of x ,

$$\bar{x} = x/|x|. \quad (3.2)$$

So $\bar{x} \in C$, where C is the simplex

$$C = \{x \in \mathbb{R}_+^2: |x| = 1\}. \quad (3.3)$$

If n is a population vector, $|n|$ equals the *total population number* and \bar{n} is the *age-structure*.

Throughout the rest of the paper we assume that the distribution of ϕ_i in Eq. (2.2) is a two-parameter gamma distribution with the density,

$$g(\phi) = \{k^a / \Gamma(a)\} \phi^{a-1} e^{-k\phi}, \quad a > 0, \quad k > 0 \quad (3.4)$$

where

$$\Gamma(a) = \int_0^\infty \phi^{a-1} e^{-\phi} d\phi \quad (3.5)$$

is the gamma function [1]. Mean and variance of this distribution are given by

$$\bar{\phi} = \mathbb{E}(\phi) = a/k; \quad \bar{\phi}^2 = \text{Var}(\phi) = a/k^2 \quad (3.6)$$

so that by choosing appropriate values of a and k we can vary $\bar{\phi}$ and $\bar{\phi}^2$ independently. This enables us to make a comparison with the numerical simulations in [8]. By the particular choice (3.4) we are able to utilize earlier results of Dyson [5] in the context of random harmonic chains and obtain the exact stationary distribution of age-structures. The applicability of Dyson's method to population models with two age-classes was first noted by Tuljapurkar [13, 14].

Under the condition $0 < f < 1$, which is assumed in the sequel unless indicated otherwise, a product of any two matrices of the form (2.2) is positive with probability one. Hence we can use the theory of random products of nonnegative i.i.d. matrices with contractive properties, see e.g. [3, 4, 7, 10, 14] and the results in [2] (in particular Corollary III.3.4, Theorem III.4.3 and Theorem V.5.1; the additional irreducibility and moment conditions are satisfied in our case).

We list the following properties, which are needed in the sequel:

$$(i) \quad \lim_{t \rightarrow \infty} \frac{1}{t} \ln |n_t| = \gamma \quad (3.7)$$

for any initial vector $n_0 \neq 0$ and almost all sequences of matrices $\{X_t\}$. The constant γ , also called the upper Lyapunov exponent, is the average long-run growth rate of the population.¹

¹ The natural logarithm is denoted by "ln"

- (ii) the process $\{\bar{n}_t\}$ is a Markov chain on the space C of age-structures; for any initial age-structure \bar{n}_0 the age-structure distribution converges to a unique μ -invariant measure ν on C , where μ is the common distribution of the matrices $\{X_t\}$ induced by the distribution (3.4).
- (iii) the logarithm of total population number obeys the central limit theorem, i.e. for some $\sigma > 0$,

$$(\sigma\sqrt{t})^{-1}\{\ln|n_t| - \gamma t\} \xrightarrow{d} N(0, 1) \quad (t \rightarrow \infty) \tag{3.8}$$

where \xrightarrow{d} denotes convergence in distribution, $N(0, 1)$ is the standard normal distribution and γ is the same as in (3.7).

- (iv) the mean γ and variance σ^2 of the long-run growth rate can be calculated as follows,

$$\gamma = \int \int \ln|X\bar{n}| \, d\mu(X) \, d\nu(\bar{n}) \tag{3.9a}$$

$$\sigma^2 = -\gamma^2 + \int \int \{\ln|X\bar{n}|\}^2 \, d\mu(X) \, d\nu(\bar{n}). \tag{3.9b}$$

Thus it appears that we need the invariant age-structure distribution $\nu(\bar{n})$ in order to calculate the integrals (3.9). This can be obtained as follows. From Eq. (1.1) we have

$$N_{1,t+1}/N_{2,t+1} = f\phi_t\{sN_{1,t}/N_{2,t} + (1-f)s\}^{-1}. \tag{3.10}$$

Instead of age-structure we consider the ratio

$$r_t = N_{1,t}/N_{2,t}. \tag{3.11}$$

Defining,

$$\tau_t = (1-f)^{-1}r_t, \quad \eta = f\{(1-f)^2s\}^{-1}, \tag{3.12}$$

(3.10) leads to

$$\tau_{t+1} = \eta\phi_t/(1 + \tau_t). \tag{3.13}$$

By demanding the invariance of the age-structure distribution under the action of (2.1), Dyson [5] showed that the stationary distribution, or rather its density $h(\tau)$ corresponding to (3.13), obeys the linear integral equation

$$h(\tau) = \int_0^\infty h(\tau')g\left(\frac{(\tau'+1)\tau}{\eta}\right)\left\{\frac{\tau'+1}{\eta}\right\} d\tau' \tag{3.14}$$

with the unique normalized solution²

$$h(\tau) = K^{-1}\tau^{a-1}(1 + \tau)^{-a} e^{-z\tau} \tag{3.15a}$$

where

$$K = \int_0^\infty d\tau \tau^{a-1}(1 + \tau)^{-a} e^{-z\tau} \tag{3.15b}$$

² In fact Dyson considered the case $a = k = n$, $n \in \mathbb{N}$, but the solution (3.15) is easily verified

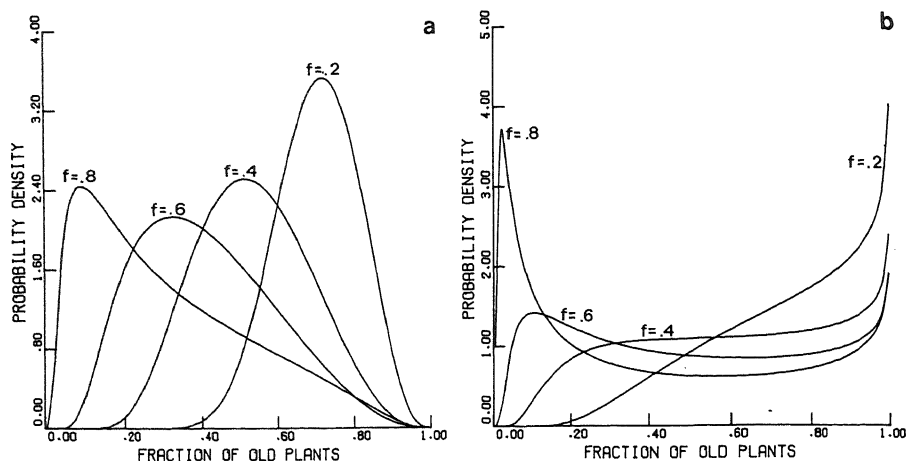


Fig. 1a b. The stationary probability density of the fraction of old plants for various values of the flowering fraction, $s = 0.9$; a $\bar{\phi} = 2$, $\bar{\phi} = 1$; b $\bar{\phi} = 2$, $\bar{\phi} = 5$

and

$$z = k/\eta = ks(1-f)^2/f. \quad (3.16)$$

The corresponding stationary density $\tilde{h}(p)$ of the fraction $p = N_2/(N_1 + N_2)$, $0 \leq p \leq 1$, of old plants is

$$\tilde{h}(p) = K'^{-1} p^{-2} (p^{-1} - 1)^{a-1} (p^{-1} - f)^{-a} e^{-z(1-f)^{-1} p^{-1}} \quad (3.17)$$

with K' the appropriate normalization constant.

In Fig. 1 we show some curves of \tilde{h} versus p for different values of the flowering fraction f , with (a) $\bar{\phi} = 2$, $\bar{\phi} = 1$, (b) $\bar{\phi} = 2$, $\bar{\phi} = 5$, the value of s being 0.9 in both cases. In case (a) the density is unimodal with the peak shifting towards larger values of p as the flowering fraction decreases. In case (b) however, the density diverges as $p \rightarrow 1$ with the local maximum near the origin disappearing as f decreases. This difference in behaviour in environments with large versus small variance of offspring number is reflected in the properties of the long-term growth rate, which is to be discussed in the following.

4. Moments of the geometric growth rate

The expression (3.9a) for the average growth rate γ specializes in our case to

$$\begin{aligned} \gamma &= \int \int \ln \left(\frac{|X(r)|}{|(r)|} \right) d\mu(X) d\nu(r) \\ &= \int_0^\infty \int_0^\infty \ln \left(\frac{f\phi + sr + (1-f)s}{r+1} \right) g(\phi) \hat{h}(r) dr d\phi \end{aligned} \quad (4.1)$$

where

$$\hat{h}(r) = (1-f)^{-1} h((1-f)^{-1}r). \quad (4.2)$$

We now use the fact that for an arbitrary random matrix $X = \begin{pmatrix} a & b \\ c & d \end{pmatrix}$ with corresponding distribution $\mu(a, b, c, d)$ and μ -invariant measure ν on \mathbb{R} and for any bounded Borel function F on \mathbb{R} , (compare [2], Sect. 2.5.2),

$$\int \int F\left(\frac{ar+b}{cr+d}\right) d\mu(a, b, c, d) d\nu(r) = \int F(r) d\nu(r). \quad (4.3)$$

Using (4.3) with $F(r) = \ln(r+1)$, $r \geq 0$, we can reduce (4.1) to a *single* integral as follows:

$$\begin{aligned} \gamma &= \int_0^\infty \int_0^\infty \left\{ \ln\left(\frac{f\phi}{sr+(1-f)s} + 1\right) + \ln(sr+(1-f)s) - \ln(r+1) \right\} g(\phi) \hat{h}(r) dr d\phi \\ &= \int_0^\infty \ln(sr+(1-f)s) \hat{h}(r) dr \end{aligned} \quad (4.4)$$

or, transforming again to the variable τ (see (3.12)),

$$\gamma(f) = \ln\{s(1-f)\} + K^{-1} \int_0^\infty \{\ln(1+\tau)\} \tau^{a-1} (1+\tau)^{-a} e^{-z\tau} d\tau. \quad (4.5)$$

Here K is the integral defined in Eq. (3.15b), and we have explicitly indicated the dependence of γ on the flowering fraction f (note that z and K also depend upon f).

The above formula (4.5) is valid for $0 < f < 1$. For $f=0$ or $f=1$ the matrix X_t in (2.2) is reducible. If $f=0$, $N_{1,t}=0$ for $t \geq 1$ and $N_{2,t}$ has a negative growth rate (assuming $N_{2,0} > 0$) given by

$$\gamma(0) = \ln s. \quad (4.6)$$

If $f=1$ it is more natural to consider time averages over *two* periods, and we find

$$\lim_{t \rightarrow \infty} \frac{1}{t} \ln(N_{i,t+2}/N_{i,t}) := 2\gamma(1), \quad i = 1, 2 \quad (4.7)$$

where

$$\gamma(1) = \frac{1}{2} \{\ln s + \mathbb{E}(\ln \phi)\} = \frac{1}{2} \{\ln(s/k) + \psi(a)\} \quad (4.8)$$

and $\psi(a) = d/da \ln \Gamma(a)$ is the digamma function [1]. The proof that the function $\gamma(f)$ as defined on the closed interval $[0, 1]$ by (4.5)–(4.8) is continuous at the endpoints of the interval will be given in Sect. 5 (that γ is continuous on $(0, 1)$ is clear from (4.5)).

We are especially concerned with the behaviour of γ as a function of the flowering fraction f . Particularly interesting is the question whether γ can have a maximum for a value $f^* < 1$ (indicating the profitability of delayed flowering) and, if so, for which values of the environmental parameters this occurs.

To answer this we have numerically evaluated the integrals in (4.5) by quadrature routines from the NAG-library.^{3,4} Again fixing s at the value 0.9 we

³ NAG-library, Fortran. Numerical Algorithms Group. Mayfield House, Oxford, U.K.

⁴ Because of the poor convergence of the integrals for small z we use the expansion (5.11) when f approaches unity

considered the following cases for the mean and variance of offspring number:

$$(a) \quad \bar{\phi} = 2, \quad \bar{\phi} = 1; \quad (b) \quad \bar{\phi} = 2, \quad \bar{\phi} = 5; \quad (c) \quad \bar{\phi} = 3, \quad \bar{\phi} = 5 \quad (4.9)$$

The results are shown as solid curves in Fig. 2. There is a clear maximum for a value $f^* < 1$ in case (b), which corresponds to the parameter range for which a similar effect was found in the simulations of Klinkhamer and de Jong [8]. Notice the very steep decrease of γ near unity (in fact $\gamma'(1) = -\infty$, as will be shown below). For comparison we also plotted the growth rate $\ln \lambda_0$ of the average population for this case, which increases monotonically with f . The maximum on $(0, 1)$ apparently tends to disappear when $\bar{\phi}$ increases (case c) or when the variance $\bar{\phi}$ decreases (case a). That this conclusion is premature is demonstrated in the next section.

We also computed the variance σ^2 of the growth rate as defined in Eq. (3.9b) by numerically evaluating

$$\sigma^2(f) = -\gamma^2(f) + \int_0^\infty \int_0^\infty \left\{ \ln \left(\frac{f\phi + sr + s(1-f)}{1+r} \right) \right\}^2 g(\phi) \hat{h}(r) dr d\phi \quad (4.10)$$

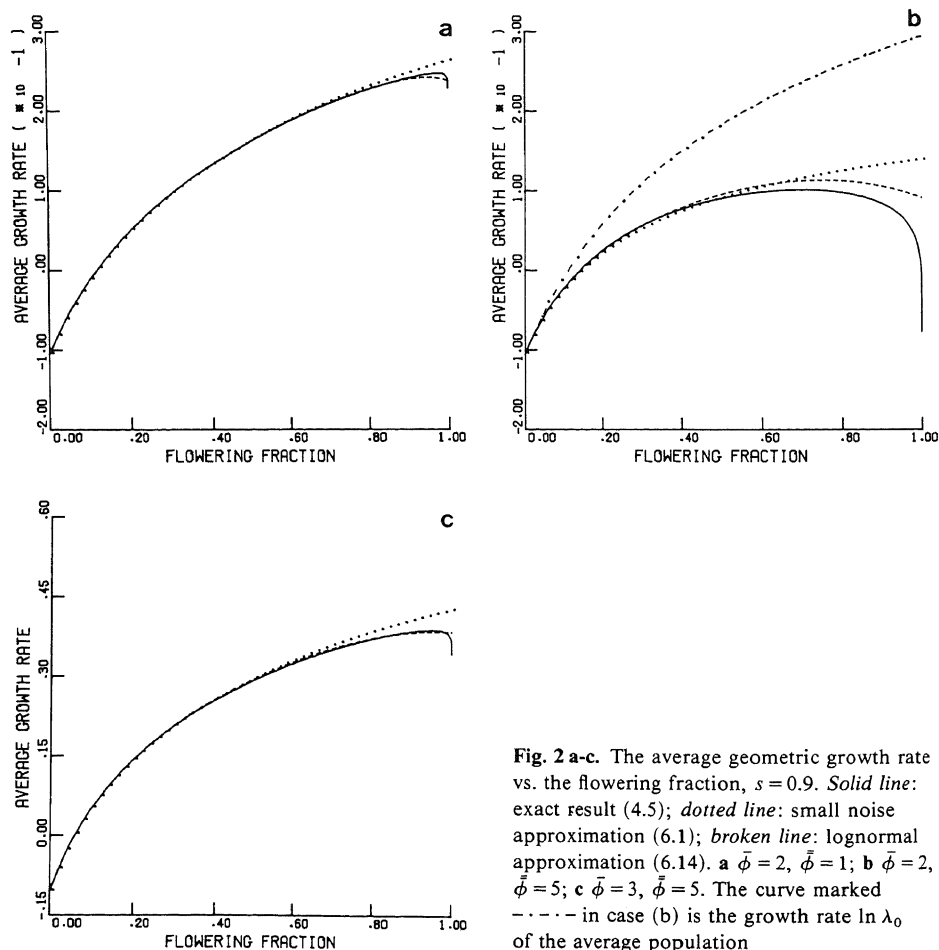


Fig. 2 a-c. The average geometric growth rate vs. the flowering fraction, $s = 0.9$. *Solid line:* exact result (4.5); *dotted line:* small noise approximation (6.1); *broken line:* lognormal approximation (6.14). **a** $\bar{\phi} = 2$, $\bar{\phi} = 1$; **b** $\bar{\phi} = 2$, $\bar{\phi} = 5$; **c** $\bar{\phi} = 3$, $\bar{\phi} = 5$. The curve marked - - - in case (b) is the growth rate $\ln \lambda_0$ of the average population

for a number of values f on $[0, 1]$, where the values at the endpoints of the interval are given by

$$\sigma^2(0) = 0 \tag{4.11a}$$

and

$$\sigma^2(1) = \frac{1}{2}[\mathbb{E}\{(\ln \phi)^2\} - \{\mathbb{E}(\ln \phi)\}^2] = \frac{1}{2}\psi'(a) \tag{4.11b}$$

where $\psi'(a)$ is the trigamma function (derivative of the digamma function). The results are shown in Fig. 3 (solid curves) for the cases (4.9). It is seen that in all cases the variance decreases steeply as the flowering fraction decreases from unity.

The tentative conclusion is that there exists indeed a parameter range, characterized by large fluctuations and/or small average of the offspring number, for which delayed flowering is profitable. The question arises as to the extent of this parameter range. To get an answer we will look at the derivative of $\gamma(f)$ at $f = 1$. This analysis will decide about the conditions for the presence of a (local) maximum *at* or *below* the value $f = 1$, respectively.

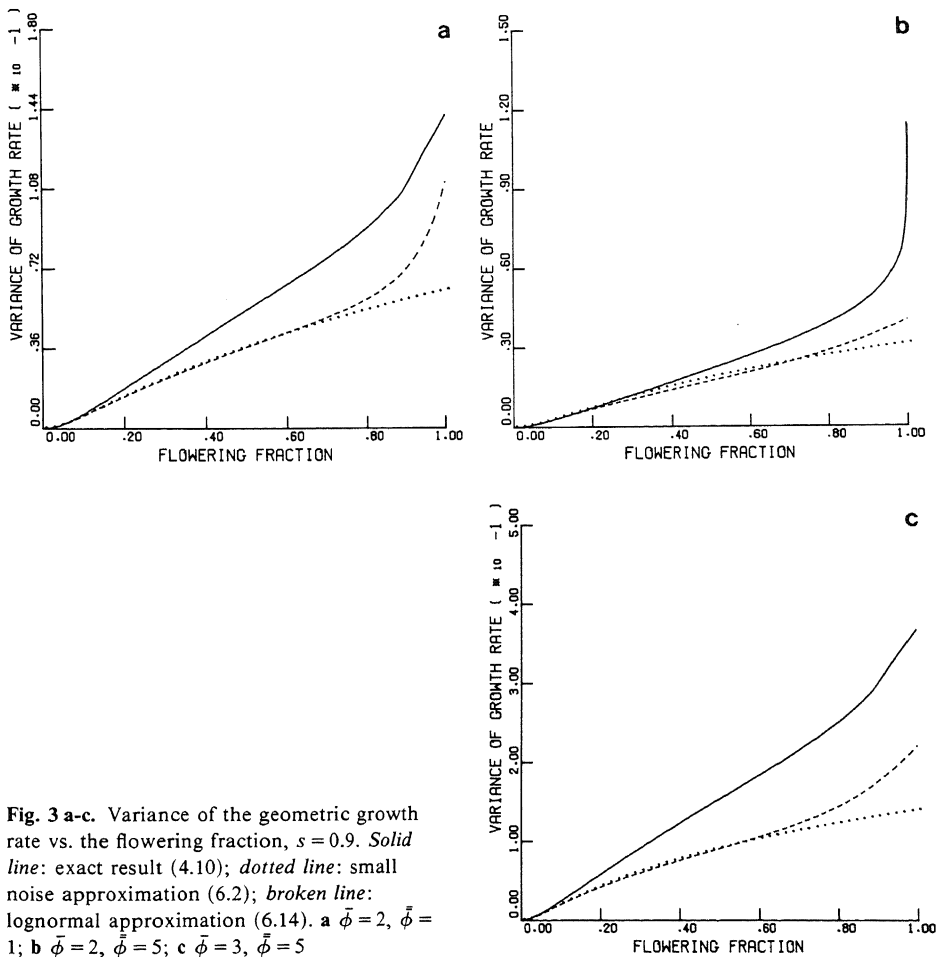


Fig. 3 a-c. Variance of the geometric growth rate vs. the flowering fraction, $s = 0.9$. *Solid line:* exact result (4.10); *dotted line:* small noise approximation (6.2); *broken line:* lognormal approximation (6.14). **a** $\bar{\phi} = 2, \bar{\phi} = 5$; **b** $\bar{\phi} = 2, \bar{\phi} = 5$; **c** $\bar{\phi} = 3, \bar{\phi} = 5$

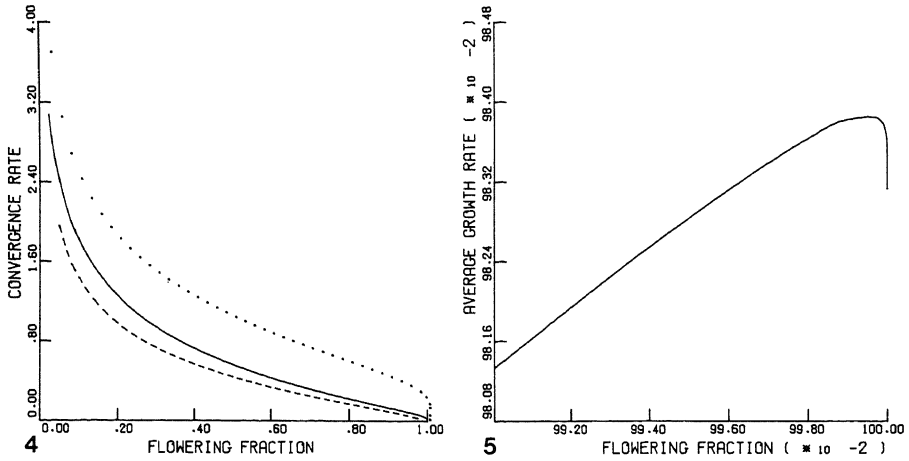


Fig. 4. Convergence rate (4.14) vs. the flowering fraction, $s = 0.9$. Solid line: $\bar{\phi} = 2, \bar{\phi} = 1$; dotted line: $\bar{\phi} = 2, \bar{\phi} = 5$; broken line: $\bar{\phi} = 3, \bar{\phi} = 5$

Fig. 5. The average geometric growth rate vs. the flowering fraction in a neighbourhood of unity, $s = 0.9, \bar{\phi} = 8, \bar{\phi} = 1$

We end this section with a remark about the rate of convergence to the stationary age-distribution. As shown in [14] the difference between initial age-structures goes to zero at least as fast as $\exp(-Rt)$, where

$$R = \gamma_1 - \gamma_2. \tag{4.12}$$

Here γ_1 and γ_2 are the largest and second largest Lyapunov exponents of the sequence $\{X_t\}$. Since the sum of the Lyapunov exponents is determined by the relation

$$\gamma_1 + \gamma_2 = \mathbb{E}\{\ln(|\det X|)\} = \ln(sf) + \mathbb{E}(\ln \phi) \tag{4.13}$$

and the exponent γ_1 equals $\gamma(f)$ as given in (4.5), it follows that

$$R(f) = -\ln f + 2\{\gamma(f) - \gamma(1)\}, \tag{4.14}$$

where we have used (4.8).

It is seen that $R(0) = \infty$ and $R(1) = 0$: convergence is very fast for f close to zero and extremely slow for f close to unity (see Fig. 4).

5. Asymptotic analysis

In this section the asymptotic behaviour of $\gamma(f)$ as $f \rightarrow 0$ or $f \rightarrow 1$ is analyzed. The first case is easy. As $f \rightarrow 0, z \rightarrow \infty$, hence it is convenient to introduce the new variable $x = z\tau$ in (4.5), yielding

$$\gamma(f) = \ln\{s(1-f)\} + \tilde{K}^{-1} \int_0^\infty \{\ln(1+\varepsilon x)\} x^{a-1} (1+\varepsilon x)^{-a} e^{-x} dx \tag{5.1a}$$

where

$$\tilde{K} = \int_0^\infty x^{a-1} (1+\varepsilon x)^{-a} e^{-x} dx \tag{5.1b}$$

and

$$\varepsilon = z^{-1} = f\{ks(1-f)^2\}^{-1}. \tag{5.2}$$

Expanding the second term in (5.1a), temporarily denoted by $S(\varepsilon)$, in powers of ε ,

$$S(\varepsilon) = \varepsilon\Gamma(a+1)/\Gamma(a) + \mathcal{O}(\varepsilon^2) \quad (\varepsilon \rightarrow 0) \tag{5.3}$$

we find

$$\gamma(f) = \ln s + (-1 + a/ks)f + \mathcal{O}(f^2) \quad (f \rightarrow 0). \tag{5.4}$$

Thus γ is indeed continuous at $f=0$ (compare Eq. (4.6)) and the slope at the origin is

$$\gamma'(0) = -1 + a/ks = -1 + \bar{\phi}/s > 0 \tag{5.5}$$

under the assumption $\bar{\phi} > s$ (see Sect. 2).

Next we look at the behaviour of γ near $f=1$. To facilitate the analysis, γ is first expressed in terms of special functions as follows.

$$\gamma(f) = \ln\{s(1-f)\} + \left[\frac{\partial}{\partial b} U(a, b, z) \right]_{b=1} / U(a, 1, z) \tag{5.6}$$

where

$$\Gamma(a)U(a, b, z) = \int_0^\infty \tau^{a-1}(1+\tau)^{b-a-1} e^{-z\tau} d\tau. \tag{5.7}$$

$U(a, b, z)$ is one of the independent solutions of Kummer's *confluent hypergeometric differential equation*, see [1], Chap. 13. It can be expressed as

$$U(a, b, z) = \frac{\pi}{\sin \pi b} \left\{ \frac{M(a, b, z)}{\Gamma(1+a-b)\Gamma(b)} - z^{1-b} \frac{M(1+a-b, 2-b, z)}{\Gamma(a)\Gamma(2-b)} \right\} \tag{5.8}$$

where $M(a, b, z)$ is the *regular* solution of Kummer's equation, having the convergent expansion (for $a > 0, b > 0$),

$$M(a, b, z) = \sum_{m=0}^\infty \frac{\Gamma(a+m)\Gamma(b)z^m}{\Gamma(a)\Gamma(b+m)m!}. \tag{5.9}$$

For $b=1$ one finds from (5.8) and (5.9) the *logarithmic* solution (see [1], Sect. 13.1.6, or the appendix),

$$\begin{aligned} -\Gamma(a)U(a, 1, z) &= M(a, 1, z) \ln z + \sum_{m=0}^\infty \frac{\Gamma(a+m)z^m}{\Gamma(a)\Gamma(1+m)m!} \\ &\quad \times \{\psi(a+m) - 2\psi(1+m)\} \end{aligned} \tag{5.10}$$

The evaluation of the derivative with respect to b occurring in (5.6) is straightforward but tedious. For the details we refer to the appendix where the following final expression for $\gamma(f)$ is obtained,

$$\gamma(f) = \frac{1}{2} \ln(sf/k) + \frac{\sum_{m=0}^\infty \frac{\Gamma(a+m)z^m}{\Gamma(1+m)m!} T_m}{2 \sum_{m=0}^\infty \frac{\Gamma(a+m)z^m}{\Gamma(1+m)m!} N_m} \tag{5.11}$$

where

$$T_m = \{2\psi(a) - \psi(a+m)\} \ln z + \{2\psi(a)(\psi(a+m) - \psi(1+m)) + 2\psi(1+m)(\psi(a+m) - \psi(a)) - \Delta(a+m)\} \quad (5.12)$$

with

$$\Delta(a) = \Gamma''(a)/\Gamma(a) \quad (5.13)$$

and

$$N_m = \ln z + \psi(a+m) - 2\psi(1+m). \quad (5.14)$$

From (5.11) one obtains the following asymptotic behaviour of $\gamma(f)$ as $f \rightarrow 1$, i.e. $z \rightarrow 0$,

$$\gamma(f) = \frac{1}{2} \ln(s/k) + \frac{1}{2} \{\psi(a) - \psi'(a)(\ln z)^{-1}\} + \mathcal{O}((\ln z)^{-2}) \quad (z \rightarrow 0) \quad (5.15)$$

with ψ' the derivative of the digamma function.

First, we note that the limiting value of $\gamma(f)$ as $f \rightarrow 1$ which follows from (5.15) coincides with the value given in Eq. (4.8), confirming the continuity of γ at $f=1$. The derivative of γ for $f \approx 1$ is also easily found from (5.15),

$$\gamma'(f) \approx -[\{2 \ln(1-f)\}^2 (1-f)]^{-1} \psi'(a) \quad (f \rightarrow 1) \quad (5.16)$$

and, taking into account that $\psi'(a) > 0$ for $a > 0$, we find

$$\gamma'(1) = -\infty. \quad (5.17)$$

This remarkable result implies that, independent of the values of the parameters a and k or, equivalently, of the mean and variance of ϕ_i , a decrease of f starting from unity will always lead initially to a larger growth rate $\gamma(f)$. From the continuity of γ and the signs of the derivatives at $f=0$ and $f=1$ it follows that $\gamma(f)$ has an absolute maximum at an *interior* point f^* , that is $0 < f^* < 1$ and $\gamma(f^*) > \gamma(1)$. The numerical results in Fig. 2 suggest that there are no other (local) maxima on $(0, 1)$. It is clear that for very large values of the mean of the offspring number or for small values of its variance, f^* lies very close to unity and the occurrence of a maximum at $f^* < 1$ can no longer be visually discerned on the scale as used in Fig. 2. For the case $\bar{\phi} = 8$, $\bar{\phi} = 1$, we have calculated $\gamma(f)$ numerically for a number of values of f in the interval $[0.99, 1.0]$, based on the expansion (5.11). The result is shown in Fig. 5. In this case there is a maximum at $f^* \approx 0.9995$ with $\gamma(f^*) = 0.9838$, whereas $\gamma(1) = 0.9831$.

6. Approximations

In this section we discuss some approximations to the moments of the growth rate and compare to the exact results.

6.1. The small noise approximation

If the variance of the offspring number is small compared to its mean one can perform a perturbation expansion of the moments of the growth rate in powers of a small parameter measuring the size of the fluctuations. Such an analysis has

been given by Tuljapukar [11] and we quote here the results for the i.i.d. case up to second order:

$$\gamma = \ln \lambda_0 - \tau^2 / (2\lambda_0^2) \quad (6.1)$$

$$\sigma^2 = \tau^2 / \lambda_0^2 \quad (6.2)$$

where λ_0 is the largest eigenvalue (2.7) of the average matrix $\mathbb{E}(X)$ and

$$\tau^2 = \{(v_0 \otimes v_0)' C_0 (u_0 \otimes u_0)\} / T_0^2 \quad (6.3)$$

with

$$T_0 = v_0' u_0. \quad (6.4)$$

Here v_0 and u_0 are the left and the right eigenvectors of $\mathbb{E}(X)$ corresponding to the eigenvalue λ_0 , primes denote transposition, \otimes denotes the Kronecker product of vectors or matrices and C_0 is the autocovariance matrix,

$$C_0 = \mathbb{E}(X \otimes X) - \{\mathbb{E}(X)\}^2. \quad (6.5)$$

In our case these formulas specialize to

$$u_0' = (1, \lambda_0 / f\bar{\phi}), \quad v_0' = (1, \lambda_0 / s), \quad (6.6)$$

hence

$$T_0 = 1 + \lambda_0^2 (f\bar{\phi}s)^{-1} \quad (6.7a)$$

and

$$C_0 = f^2 \bar{\phi} \left\{ \begin{pmatrix} 0 & 1 \\ 0 & 0 \end{pmatrix} \otimes \begin{pmatrix} 0 & 1 \\ 0 & 0 \end{pmatrix} \right\}. \quad (6.7b)$$

Inserting (6.6)–(6.7) in (6.3) we find

$$\tau^2 = \lambda_0^2 \bar{\phi} [\bar{\phi}^2 \{1 + \lambda_0^2 (f\bar{\phi}s)^{-1}\}^2]^{-1}. \quad (6.8)$$

The small noise approximation (6.1) for the mean growth rate is plotted in Fig. 2 as the dotted line. The accuracy of the approximation depends on $\bar{\phi}$, $\bar{\phi}$ and on f . As a measure of the fluctuations one may take the quantity

$$\varepsilon = \frac{\sqrt{\|\text{Cov}(X)\|}}{\|\mathbb{E}(X)\|} = \frac{f\sqrt{\bar{\phi}}}{(2-f)s + f\bar{\phi}} \quad (6.9)$$

where we used the matrix norm $\|X\| = \sum_{i,j} |X_{ij}|$. The figures show that the approximation is accurate as long as $\varepsilon \leq 0.3$: in the cases (a) and (c) the agreement is close over almost the whole interval, whereas in case (b) the approximation becomes increasingly inaccurate as f approaches unity. The corresponding approximation for the variance σ^2 is plotted in Fig. 3, also showing increasing deviation from the exact result as f increases.

6.2. The lognormal approximation

The central limit theorem (3.8) can be loosely interpreted as saying that for large time the probability density $p(|n|, t)$ of total population number is approximately

lognormal,

$$p(|n|, t) \approx q(|n|, t)$$

where

$$q(x, t) = (2\pi\sigma^2 t)^{-1/2} x^{-1} \exp\left[-\frac{\{\ln(x/x_0) - \gamma t\}^2}{2\sigma^2 t}\right]. \quad (6.10)$$

The mean and variance of the lognormal distribution (6.10) are

$$\mathbb{E}(x_t) = x_0 \exp\{(\gamma + \frac{1}{2}\sigma^2)t\} \quad (6.11a)$$

$$\text{Var}(x_t) = x_0^2 [\exp\{2(\gamma + \frac{1}{2}\sigma^2)t\}] [\exp(\sigma^2 t) - 1] \quad (6.11b)$$

and its median is

$$\text{Med}(x_t) = x_0 \exp(\gamma t). \quad (6.12)$$

Hence if $|n_t|$ was exactly lognormal, the average geometric growth rate γ would coincide with the growth rate of the median population. In terms of the asymptotic growth rates μ_0 and μ_1 of the mean and variance of total population number, i.e.

$$\lim_{t \rightarrow \infty} \frac{1}{t} \ln \mathbb{E}(|n_t|) := \mu_0, \quad \lim_{t \rightarrow \infty} \frac{1}{t} \ln \text{Var}(|n_t|) := \mu_1, \quad (6.13)$$

one arrives at the following approximations to γ and σ^2 by comparing (6.11) and (6.13),

$$\gamma \approx 2\mu_0 - \frac{1}{2}\mu_1, \quad \sigma^2 \approx \mu_1 - 2\mu_0. \quad (6.14)$$

The argument just given is essentially reproduced from Tuljapurkar [11].

It is easy to calculate μ_0 and μ_1 in our case of independent fluctuations. In fact,

$$\mu_0 = \ln \lambda_0 \quad (6.15)$$

where λ_0 is the largest eigenvalue (2.7) of the average matrix $\mathbb{E}(X)$. The second moment of $|n_t|$ grows asymptotically as

$$\mathbb{E}(|n_t|^2) \sim \text{const. } \lambda_1^t$$

where λ_1 is the largest eigenvalue of the 4×4 matrix $\mathbb{E}(X \otimes X)$. Since $\lambda_1 \geq \lambda_0^2$ by positivity of the variance, we thus have from (6.13)

$$\mu_1 = \ln \lambda_1. \quad (6.16)$$

We have numerically computed λ_1 for various values of the flowering fraction f and thus constructed approximations to γ and σ^2 via (6.14)–(6.16). The results are indicated by the broken lines in Figs. 2 and 3. The approximations to the average growth rate deviate from the exact ones as f approaches unity, especially in case (b). In contrast with the small noise approximation, the lognormal approximation does yield a local maximum for a flowering fraction below unity. Notice however that in case (b) it fails to reproduce the steep decrease of γ towards a *negative* value at $f = 1$. The results for the variance are only accurate for small f , although they are better than those of the small noise approximation.

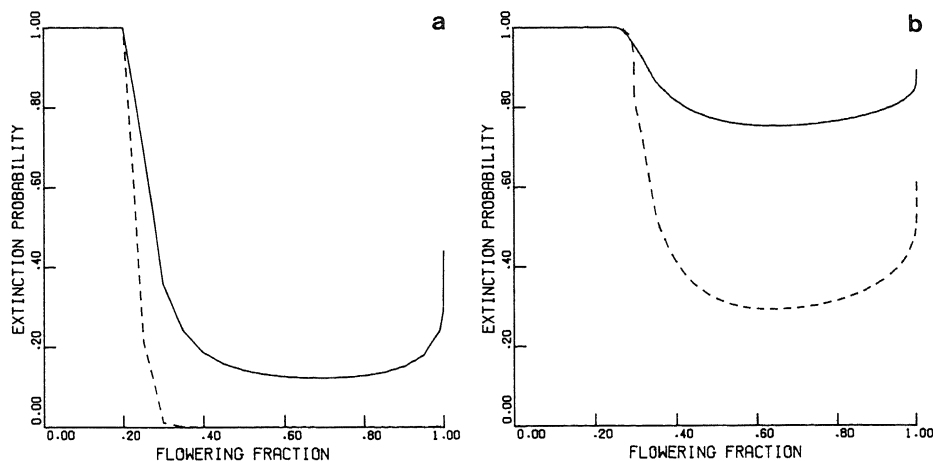


Fig. 6 a b. Extinction probability vs. the flowering fraction for initial population numbers $|n_0| = 2$ (solid line) and $|n_0| = 20$ (broken line), $s = 0.9$. a $\bar{\phi} = 2, \tilde{\phi} = 1$; b $\bar{\phi} = 2, \tilde{\phi} = 5$

7. Extinction

To discuss extinction for the model (2.1) it is customary to impose an extinction boundary at an arbitrary low level of total population number, say at $|n_t| = 1$. Using the asymptotic lognormality of the total population one can derive the following approximate results for the probability $Q(\infty)$ that the population will be eventually extinct [10],

$$Q(\infty) = \begin{cases} 1 & \gamma \leq 0 \\ \exp\left(-\frac{2\gamma}{\sigma^2} \ln|n_0|\right) & \gamma > 0. \end{cases} \quad (7.1)$$

By making use of the numerical results for γ and σ^2 discussed earlier we have plotted $Q(\infty)$ in Fig. 6 for two initial population numbers, viz. $|n_0| = 2$ and $|n_0| = 20$, respectively. The results give an indication about the behaviour of the extinction probability as a function of the flowering fraction. Notice the steep decrease of $Q(\infty)$ as f falls just below unity after which a plateau value is reached which extends over a considerable region. From a comparison of Figs. 2 and 6 it is also evident that the value of the flowering fraction maximizing the growth rate γ will in general be larger than the value which minimizes the extinction probability.

The conclusion is that delayed flowering not only increases the geometric growth rate of the population but also decreases its extinction probability, in agreement with the simulation results of [8].

8. Summary and conclusions

A model of biennial plant population with two age classes growing in a random environment is studied. The first class is formed by the individuals up to one year old who cannot flower, whereas the second class consists of individuals older than one year of which a fraction f flowers each year. If $f < 1$ one speaks

of delayed flowering and the question is whether such a delay can be profitable for the population.

To answer this question we calculate the mean γ and variance σ^2 of the geometric growth rate of the population exactly in terms of definite integrals, assuming a two-parameter gamma distribution for the randomly fluctuating number of offspring per flowering plant. From a numerical evaluation of the integrals it is found that for various values of the mean $\bar{\phi}$ and variance $\bar{\phi}^2$ of offspring number the mean growth rate γ has an absolute maximum for a value of f smaller than unity. An asymptotic analysis reveals that actually such a maximum for a value f^* strictly smaller than unity *always* occurs, although for large values of the ratio $\bar{\phi}/\bar{\phi}^2$ the value f^* is for all practical purposes identical to unity. Thus delayed flowering increases the geometric growth rate of the population. The results of some common approximations to γ and σ^2 are compared to the exact results. Finally it is shown that delayed flowering decreases the extinction probability of the population.

Acknowledgements. We thank Peter Klinkhamer and Tom de Jong for extensive discussions on the biological aspects of the model and Nico Temme for helpful advice concerning the numerical computations and the special functions occurring in this paper.

Appendix

The starting point in the derivation of Eq. (5.11) is Eq. (5.6). Define

$$W(b) := \Gamma(a)U(a, b, z) = \pi R(b)/\sin \pi b \quad (\text{A.1})$$

with (see (5.8)),

$$R(b) = h(b) - z^{1-b}g(b) \quad (\text{A.2})$$

and

$$h(b) = \frac{M(a, b, z)\Gamma(a)}{\Gamma(1+a-b)\Gamma(b)}, \quad g(b) = \frac{M(1+a-b, 2-b, z)}{\Gamma(2-b)}. \quad (\text{A.3})$$

Noting that both the numerator and the denominator in (A.1) are zero as $b \rightarrow 1$, we compute the limit of $W(b)$ as $b \rightarrow 1$ by l'Hôpital's Rule with the result,

$$W(1) = -R'(1) = -\{h'(1) - g'(1) + g(1) \ln z\}, \quad (\text{A.4})$$

primes denoting differentiation *w.r.t.* b . The next quantity to be computed is $W'(1)$. From (A.1) one has

$$W'(b) = \pi\{-\cos \pi b W(b) + R'(b)\}/\sin \pi b. \quad (\text{A.5})$$

Again the numerator and denominator of (A.5) are zero as $b \rightarrow 1$, so another application of l'Hôpital's Rule yields

$$W'(1) = \left[\frac{\pi\{-\pi \sin \pi b W(b) - \cos \pi b W'(b) + R''(b)\}}{\pi \cos \pi b} \right]_{b=1} \quad (\text{A.6})$$

from which it follows that

$$W'(1) = -\frac{1}{2}R''(1) = -\frac{1}{2}\{h''(1) - g''(1) + 2g'(1) \ln z - g(1)(\ln z)^2\}. \quad (\text{A.7})$$

From (A.4) and (A.7) we see that the second term in (5.6) is singular as $z \rightarrow 0$, i.e. $f \rightarrow 1$. The same holds for the first term in (5.6) and in fact the two singularities cancel to give a finite result as $f = 1$.

To show this we first deduce from the definition (3.16) of z that

$$\ln z = \ln(ks/f) + 2 \ln(1-f). \quad (\text{A.8})$$

Inserting this in (5.6) and using (A.4) and (A.7) we obtain

$$\begin{aligned} \gamma(f) &= \frac{1}{2} \ln(sf/k) + \frac{1}{2} \ln z + \frac{1}{2} R''(1)/R'(1) \\ &= \frac{1}{2} \ln(sf/k) + \frac{1}{2} \left[\frac{\{h'(1) + g'(1)\} \ln z + h''(1) - g''(1)}{h'(1) - g'(1) + g(1) \ln z} \right]. \end{aligned} \quad (\text{A.9})$$

It remains to evaluate the derivatives of h and g . Tedious but elementary calculation yields

$$g(1) = \{\Gamma(a)\}^{-1} \sum_{m=0}^{\infty} \frac{\Gamma(a+m)z^m}{\Gamma(1+m)m!} = M(a, 1, z) \quad (\text{A.10})$$

$$h'(1) + g'(1) = \{\Gamma(a)\}^{-1} \sum_{m=0}^{\infty} \frac{\Gamma(a+m)z^m}{\Gamma(1+m)m!} \{2\psi(a) - \psi(a+m)\} \quad (\text{A.11})$$

$$h'(1) - g'(1) = \{\Gamma(a)\}^{-1} \sum_{m=0}^{\infty} \frac{\Gamma(a+m)z^m}{\Gamma(1+m)m!} \{-2\psi(1+m) + \psi(a+m)\} \quad (\text{A.12})$$

$$\begin{aligned} h''(1) - g''(1) &= \{\Gamma(a)\}^{-1} \sum_{m=0}^{\infty} \frac{\Gamma(a+m)z^m}{\Gamma(1+m)m!} \{-4\psi(a)\psi(1+m) + 2\psi(a)\psi(a+m) \\ &\quad + 2\psi(a+m)\psi(1+m) - \Delta(a+m)\} \end{aligned} \quad (\text{A.13})$$

where $\psi(a) = d/da \ln \Gamma(a)$ and $\Delta(a)$ is defined in (5.13). Insertion of (A.10)–(A.13) in (A.9) yields the desired results (5.11)–(5.14).

References

1. Abramowitz, M., Stegun, I. A.: Handbook of mathematical functions. Natl. Bur. Standards U.S.A., Washington (1972)
2. Bougerol, P., Lacroix, J.: Products of random matrices with applications to Schrödinger operators (in Progress in Probability and Statistics, Vol. 8) Part A, Boston; Birkhäuser 1985
3. Cohen, J. E.: Ergodicity of age-structure in populations with Markovian vital rates. II. General states. Adv. Appl. Probab. **9**, 18–37 (1977)
4. Cohen, J. E.: Ergodic theorems in demography. Bull. Am. Math. Soc. **3**, 275–295 (1979)
5. Dyson, F. J.: The dynamics of a disordered linear chain. Phys. Rev. **92**, 1331–1338 (1953)
6. Hart, R.: Why are biennials so few? Am. Natur. **111**, 792–799 (1977)
7. Heyde, C. C., Cohen J. E.: Confidence intervals for demographic projections based on products of random matrices. Theor. Popul. Biol. **27**, 120–153 (1985)
8. Klinkhamer, P. G. L., de Jong T. J.: Is it profitable for biennials to live longer than two years? Ecol. Modell. **20**, 223–232 (1983)
9. Random matrices and their applications. (Contemporary Mathematics, vol. 50) Cohen, J. E., Kesten, H., Newman, C. M. (eds.) A.M.S., Providence 1986
10. Tuljapurkar, S. D., Orzack, S. H.: Population dynamics in variable environments. I. Long-run growth rate and extinction. Theor. Popul. Biol. **18**, 314–342 (1980)
11. Tuljapurkar, S. D.: Population dynamics in variable environments. II. Correlated environments, sensitivity analysis and dynamics. Theor. Popul. Biol. **21**, 114–140 (1982)
12. Tuljapurkar, S. D.: Population dynamics in variable environments. III. Evolutionary dynamics of r-selection. Theor. Popul. Biol. **21**, 141–165 (1982)
13. Tuljapurkar, S. D.: Demography in stochastic environments. I. Exact distributions of age-structure. J. Math. Biol. **19**, 335–350 (1984)
14. Tuljapurkar, S. D.: Demography in stochastic environments. II. Growth and convergence rates. J. Math. Biol. **24**, 569–581 (1986)
15. Van der Meijden E., Van der Waals-Kooi, R. E.: The population ecology of *Senecio jacobaea* in a sand dune system. I. Reproductive strategy and the biennial habit. J. Ecol. **67**, 131–153 (1979)

Received June 22/ Revised October 13, 1987

Note added in proof. S. D. Tuljapurkar correctly pointed out to the author that Eq. (3.9b) is not an exact expression for the variance. All results based upon this equation are therefore of limited validity.